

Mechanical Properties of Basalt Filaments

Abstract

In this contribution selected physical and mechanical properties of laboratory prepared basalt filaments and fibres drawn out from these are presented. The mechanical properties were investigated after tempering up to 800 °C. The ultimate strength distribution, torsional rigidity, deformation at break and sound wave spread velocity are mentioned. The thermal properties were investigated by TMA apparatus. The thermal expansion and compressive creep were measured. Analysis of a fibrous fragment evolved during the abrasion of basalt weave is presented. Basalt particles are too thick to be directly respirable, but their length/diameter ratio is higher than 3 and therefore the handling of basalt fibres must be carried out with care.

Key words: basalt filaments, mechanical properties, thermo-mechanical properties, compressive creep, fibrous fragment analysis.

tion of some structural parts (plagioclase, magnetite, pyroxene) and due to the non-homogeneity of melt. Utilisation of the technology of continuous spinning overcomes the problem of unevenness and the resulting filament yarns are applicable in the textile branch. It is possible to use these yarns for the production of planar or 3D textile structures for composites, special knitted fabrics and also as the sewing threads. The application of basalt yarns as sewing threads is especially attractive. It is possible to use these threads for the joining of filtering bags for hot media, and for very aggressive chemical environments, etc.

In this contribution selected properties of basalt filaments are presented. As starting material the laboratory prepared filaments were used by us. Mechanical properties were investigated at room temperature, and then tempered to 50, 100, 200, 300, 400, 500 °C, and in some experiments up to 800 °C. The analysis of the fibrous fragment evolved during the abrasion of basalt weave is presented.

Basalt fibres

Basalt is the generic name for solidified lava which has poured out of volcanoes [1, 2, 5]. Basaltic rocks melts approximately within the range of 1,500 - 1,700 °C. A Glass like, nearly amorphous solid is the result of quickly quenched melt. Slow cooling leads to more or less complete crystallisation, and then to an assembly of minerals. Two essential minerals: plagiocene and pyroxene make up perhaps 80% of many types of basalt. Classification of basaltoid rocks, based on the content of main basic minerals, is described in the book [5]. As far as the chemical composition of basalt is concerned, the silicon oxide SiO₂ (optimal range

Table 1. Basic physical properties of glass and basalt fibres.

Property	E-glass	basalt
Diameter, µm	9 - 13	12.96
Density, kgm ⁻³	2540	2733
Softening temperature, °C	840	960

43.3 - 47%) dominates and Al₂O₃ (optimal range 11 - 13%) is next in abundance. The content of CaO (optimal range 10 - 12%) and MgO (optimal range 8 - 11%) is very similar. Other oxides are almost always below the level of 5%.

According to our previous findings, it was proved that the stability of basalt in alkalis is generally very good. However, stability in acids is comparatively small. Prolonged acid activity leads to the full disintegration of fibres.

The aim of the work presented in this paper was to determinate the properties of basalt fibres prepared in laboratory conditions from 'Kamenniy Vek' Russian basalt rods by a particularly innovative method proposed by us for testing basalt fibres. The investigations were carried out before and after thermal exposition, and it was also better to include a thermo-mechanical analysis. Additionally, the particle emitted during the handling of basalt fibres were also analysed.

Materials

Basalt rocks from KAMENNIY VEK - Russia were used as a raw material in this work. Marble and filament roving were prepared by us under laboratory conditions. From marble thick rods were prepared by grinding. The roving contained 952 single filaments. The mean fineness of the roving was 320 tex. The

Introduction

Basalt materials are attractive for the creation of composites with polymeric and inorganic matrices. The main advantages are low price of raw materials, cheap production of filaments and possibilities for the creation of textile structures (weaves, knitted forms etc.).

Basalt products can be used at very low temperatures (about -200 °C) up to comparatively high temperatures of 700 - 800 °C. At higher temperatures structural changes occur. It is possible to use some dopes for the increasing or enhancing of Basalt properties as well.

The main problems of basalt fibre preparation are due to the gradual crystallisa-

basic physical properties of basalt fibres are presented in Table 1.

Statistical Analysis of Fibres Strength

The fracture of fibres can be generally described by micro mechanical models or on the basis of pure probabilistic ideas [8]. The probabilistic approach is based on these assumptions:

- 1 fibre breaks at a specific place with critical defect (catastrophic flaw),
- 2 defects are distributed randomly along the length of fibre (model of Poisson marked process),
- 3 fracture probabilities at individual places are mutually independent.

The cumulative probability of fracture $F(V, \sigma)$ depends on the tensile stress level and fibre volume V . The simple derivation of the stress at break distribution described for example by Kittl and Diaz [9] leads to the general form

$$F(V, \sigma) = 1 - \exp(-R(\sigma)) \quad (1)$$

The $R(\sigma)$ is known as the specific risk function. For Weibull distribution function $R(\sigma)$ has the form [14]

$$R(\sigma) = [(\sigma - A)/B]^C \quad (2)$$

Here A is the lower strength limit, B is the scale parameter and C is the shape parameter. For brittle materials it is often assumed that $A = 0$.

Weibull models are physically incorrect due to an unsatisfactory upper limit of strength.

Kies proposed a more realistic risk function in the form

$$R(\sigma) = \left(\frac{\sigma - A}{A1 - \sigma} \right)^C \quad (3)$$

Here $A1$ is the upper strength limit. For brittle materials it can also be assumed that $A = 0$. Further generalisation of $R(\sigma)$ has been published by Phani

$$R(\sigma) = \frac{\left(\frac{\sigma - A}{B1} \right)^D}{\left(\frac{A1 - \sigma}{B} \right)^C} \quad (4)$$

It can be proved that B and $B1$ cannot be independently estimated. Therefore the constraint $B1 = 1$ is used in sequel. The simplified version of eqn. (4) has $A = 0$.

For the well known Gumbell distribution $R(\sigma)$ in described as

$$R(\sigma) = e^{-\frac{\sigma - l}{B}} \quad (5)$$

The main aim of the statistical analysis is the specification of $R(\sigma)$ and parameter estimation based on the experimental strengths $\sigma_i, i = 1, 2, \dots, N$. Based on the preliminary computation, it was determined that the Weibull distribution is suitable for basalt fibre strength.

The individual basalt fibres removed from roving were tested. The loads at break were measured under standard conditions at a sample length of 10 mm. The Load data were transformed into stresses at break σ_i in GPa. A sample of 65 stresses at break values was used for evaluation of the $R(\sigma)$ functions and estimate of their parameters.

Rearrangement of eqn. (3) leads to the form

$$y(\sigma) = \ln[R(\sigma)] \quad (6)$$

where $y(\sigma) = \ln[-\ln(1-F(\sigma))]$. $F(\sigma)$ is the distribution function.

For further simplification the so called strength rank statistics $\sigma_{(i)}$ can be used, which denote that $\sigma_{(i)} \leq \sigma_{(i+1)}, i = 1, 2, \dots, N-1$ [10]. $\sigma_{(i)}$ values are rough estimates of the strength quantile function for probabilities

$$p_i = F(\sigma_{(i)}) = \frac{i - 0.5}{N + 0.25} \quad (7)$$

Parameter estimates of $R(\sigma)$ models can then be obtained by nonlinear least squares i.e. by the minimising of criterion

$$S = \sum_{i=1}^N [y(\sigma_{(i)}) - \ln R(\sigma_{(i)})]^2 \quad (8)$$

Due to the roughness of $\sigma_{(i)}$ and their no constant variances special weights can be defined [7]. Transformation of parameter estimation problems in $R(\sigma)$ models into a regression problem enables use of statistical criteria for selection of the optimal model form. The most suitable is Akaike information criterion AIC, defined as [11]

$$AIC = N \cdot \ln \left(\frac{S^*}{N} \right) + 2M \quad (9)$$

Here M is the number of parameters estimated and S^* is the minimal value of S (see eqn. (8)). Another possibility is the estimation of strength probability density function $f(\sigma) = F'(\sigma)$ parameters by the maximum likelihood method.

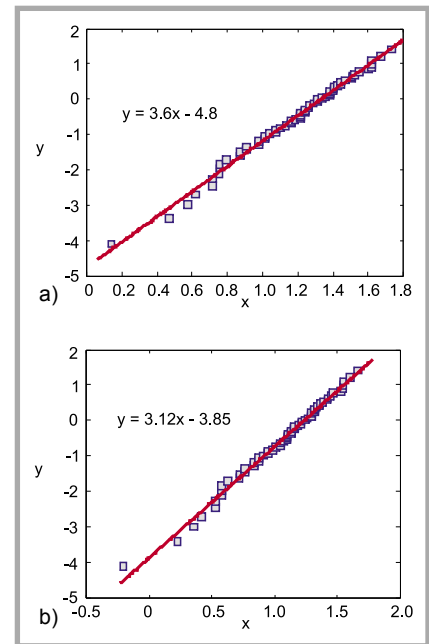


Figure 1. Weibull Q-Q plot for a) two parameter case and b) three parameter case.

The simple graphical method for the checking of Weibull distribution suitability is based on the so called Q-Q plot, which is a comparison of experimental strength quantiles $\sigma_{(i)}$ and Weibull model quantiles. After rearrangements of the linear dependence, $y = a \times x + b$ in Q-Q plot occurs.

For two parameters Weibull distribution is:

$$y = \ln[-\ln(1-p_i)], x = \ln(\sigma_{(i)}), a = C \text{ and } b = -\ln(B) \times C.$$

This Q-Q graph is shown in Figure 1.a. From the parameters of the regression line we can observe that shape parameter $B = 3.796$ and scale parameter $C = 3.6$.

For three parameter Weibull distribution is:

$$y = \ln[-\ln(1-p_i)], x = \ln(\sigma_{p(i)} - A), a = C \text{ and } b = -\ln(B) \times C.$$

In this case it is necessary to know the estimator of lower strength limit A . One simple possibility is to use the moment estimator $A = 0.3391$ obtained from eqn. (11). This Q-Q graph is shown on the Figure 1.b. From the parameters of the regression line we can observe that shape parameter $B = 3.435$ and scale parameter $C = 3.12$.

For quick and rough parameter estimates of three parameter Weibull models the moment based method can be used. The main idea of this method is very sim-

ple. Based on sample m , moments and corresponding theoretical moments for selected strength distribution nonlinear equations m can be created. Their complexity is based on the suitable selection of moments [10].

Cran [15] used this technique for the estimation of the parameters in three parameter Weibull distribution. Shape parameter C can be estimated from relation

$$C = \frac{\ln(2)}{\ln(m_3 - m_2) - \ln(m_2 - m_1)} \quad (10)$$

For estimation of the lower limit, strength A is valid

$$A = \frac{m_1 m_2 - m_2^2}{m_1 + m_2 - 2m_2} \quad (11)$$

and an estimate of scale parameter B is in the form

$$B = \frac{m_1 - A}{\Gamma\left(1 + \frac{1}{C}\right)} \quad (12)$$

where $\Gamma(x)$ is the Gamma function. In relations m_r so-called Weibull sample moments are special, defined as

$$m_r = \sum_{i=0}^{m-1} \left(1 - \frac{i}{N}\right)^r \left[E_{(1-i/N)} - x_{(0)} \right] \quad (13)$$

For $i = 0$ is formally $x_{(0)} = 0$.

This very simple technique can be used for the rough estimation of strength distribution parameters. It is suitable for prediction of the importance of parameter A in Weibull models [15]. For a two parameter Weibull model is $A = 0$ and C is estimated from relation

$$C = \frac{\ln(2)}{\ln(m_3) - \ln(m_2)} \quad (14)$$

The assumption $A=0$ is valid if the B and C estimates for two and three parameter Weibull models are reasonably close.

For experimental data we have the following moment estimators: $A = 0.3391$, $B = 3.4121$ and $C = 3.3297$. The closeness between parameters obtained from Q-Q plot and by using of moments is acceptable. The advantage of Q-Q plot is that it allows inspection of all points and identify outliers. The differences between three and two parameter Weibull distributions are, in light of the data, negligible.

The SEM of the longitudinal portion of broken fibre (magnification 10 000) demonstrates that the surface is very smooth without flaws or crazes (see Figure 2.a). Based on these findings we can

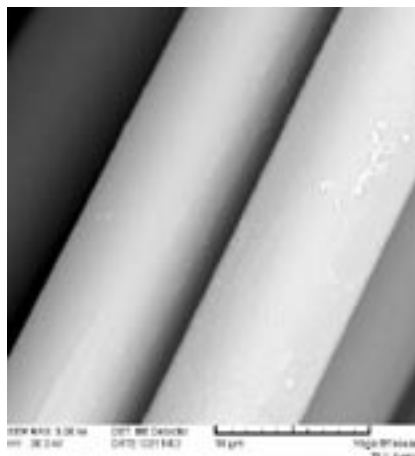


Figure 2.a. A longitudinal view of basalt fibre.

postulate that fracture occurs due to non homogeneities in fibre volume (probably near the small crystallites of minerals, see Figure 2.b).

Basalt fibre properties after thermal exposition

The behaviour of basalt fibres after long-term thermal exposition was simulated by the tempering of fibres at the selected temperatures for the chosen time of exposition. Three sets of experiments were applied.

In the first set of experiments, the thermal exposition influence on the ultimate mechanical properties and dynamic acoustical modulus of basalt filament roving for tempering temperatures of 50, 100, 200, 300, 400 and 500°C was evaluated. The time of exposition was 60 min. After the tempering the following properties were measured:

- Tensile strength, cN.tex⁻¹.
- Deformation at break, %.
- Dynamic acoustic modulus, Pa.

The dynamic acoustic modulus was determined from the sound wave spread velocity in the material.

The changes in the properties of basalt fibres after tempering were investigated by the analysis of variance. It was determined that tempering at 300 °C and higher led to a statistically significant drop in strength and dynamic acoustic modulus. Probably, the changes in these properties are due to changes in the crystalline structure of the fibres.

In the second set of experiments the strength distribution of basalt filament

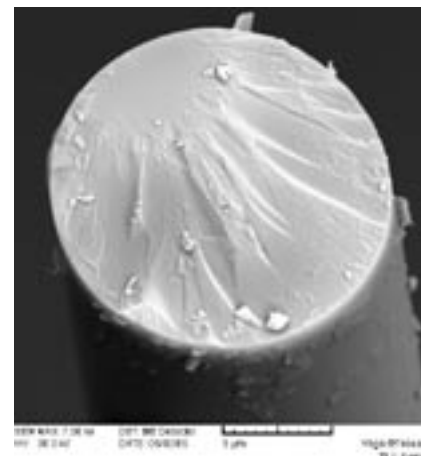


Figure 2.b. A view of broken basalt fibre – A typical cross-section of brittle failure.

roving was measured for samples tempered in an oven at temperatures $T_T = 20, 50, 100, 200, 300, 400$ and 500 °C at time intervals $t_T = 15$ and 60 min. For roving strength measurements a TIRATEST 2300 machine was used. 50 samples of strengths P_i were collected. These values were recalculated as stress at break values σ_i in GPa.

The strength distribution of tempered multifilament roving was nearly Gaussian with parameters mean σ_p and variance s^2 . These parameters were estimated from a sample arithmetic mean and sample variance.

The dependence of roving strength on temperature exhibits two nearly linear regions. One at the low temperature of 180 °C with nearly constant strength, and one up to 340 °C with a very fast strength drop.

To describe of this dependence, a linear spline model was used [11]. The strengths σ_1 for temperature $T_1=180$ °C and σ_2 for temperature $T_2 =340$ °C were computed using the least linear least squares. These values and the rate of strength drop $Ds = (\sigma_1 - \sigma_2)/160$ in GPa deg⁻¹ are given in Table 2.

It is clear that increasing the time of tempering leads to the acceleration of structural changes and drops in strength fastening (increasing Ds).

Table 2. Parameters of dependence of roving strength on temperature.

t_T , min	σ_1 , GPa	σ_2 , GPa	Ds , GPa deg ⁻¹
15	1.1070	0.343	0.0048
60	1.1750	0.158	0.0064

Table 3. Shear modulus of basalt fibres.

T _T , °C	t _T , min	G, GPa
-	-	21.76
100	15	19.43
100	60	11.34
250	15	18.04
250	60	12.76

In the third set of experiments the influence of thermal exposition on shear modulus was investigated. The individual basalt filaments removed from roving were tested. Apparatus based on the torsion pendulum principle was used. In this apparatus a fibre of length l_0 is hung with a pendulum (moment of inertia M) and subjected to a small shear strain imposed by a small initial twist. The period P and amplitude A of successive oscillations were measured. The shear modulus of circular fibre of radius r is.

$$G = \frac{2I_0 M \omega^2}{\pi r^4} \quad (15)$$

where frequency of oscillations is in the form

$$\omega = \frac{2\pi}{P} \quad (16)$$

For the pendulum a cylindrical disc of radius R and mass m was used. The corresponding moment of inertia is

$$M = 1/2 m R^2 \quad (17)$$

The shear modulus computed for tempering temperatures T_T and time of exposures t_T are in Table 3 (see page 54).

The shear modulus is comparatively high. The prolongation of tempering leads to the high drop of G .

■ Thermomechanical analysis

In thermo-mechanical analysis (TMA) the dimensional changes (expansion or contraction) are measured under defined load and chosen time. TMA requires high-resolution measurement of linear displacement and excellent stability of measured conditions. Most TMA instruments on the market are not sensitive to very small displacements. This was the main reason for construction of a special device TMA CX 03RA/T at the University of Pardubice. This device was developed to provide a highly sensitive tool for reproducible measurement of subtle dimensional changes even at extremely long thermal expositions. The sample is placed on a movable sample holder connected to a displacement sensor,

which measures dimensional changes in the sample. A detailed description of this instrument is in [3].

The instrument is fully computer controlled with programmable time - temperature profiles and allows loading in static or dynamic mode. Special adapters for the application of this instrument for bending and tension deformations are now under preparation. The apparatus described were/has been used for all kinds of measurements. Basalt rods (abbreviation R) and linear composite from roving, glued by epoxy resin CHS 1200 (abbreviation C), were used.

Dilatation curves, i.e., dependence of the height of the basalt rod on the temperature, were measured at a rate of heating of 10 deg min⁻¹ and compressive load of 10 mN. These curves consist of two nearly linear portions connected at glass transition temperature T_g [3].

The coefficients of linear thermal expansions a for the region below and above T_g were computed from models

$$L = L_g + a_1 \cdot (T - T_g) \text{ for } T < T_g \quad (18)$$

$$L = L_g + a_2 \cdot (T - T_g) \text{ for } T > T_g \quad (19)$$

From the nonlinear least squares:

$$T_g = 596.3 \text{ }^\circ\text{C}, a_1 = 4.9 \cdot 10^{-6} \text{ deg}^{-1}, a_2 = 19.1 \cdot 10^{-6} \text{ deg}^{-1} \text{ were computed.}$$

The responses of basalt on the compressive loads under isothermal conditions were investigated from creep type experiments. The load was 200 mN. For the basalt rods and linear composites the dependence of sample height L for time t were measured. The experimental data

were described by the simple exponential type model [12]

$$L = L_p + L_1 e^{-k_1 t} + L_2 e^{-k_2 t} \quad (20)$$

Parameters L_p, L_1, L_2, k_1 and k_2 were estimated by using nonlinear least squares. The maximum dilatation

$$D = L_1 + L_2 \quad (21)$$

and half time of dilatation $t_{1/2}$ were computed. Note that $t_{1/2}$ is the time for dilatation equal to $L_p + (L_1 + L_2)/2$. These parameters are given in Table 4.

From compressive creep data the longitudinal compressive modulus was predicted in the following way. You take a linear composite (index C), consisting of the phase of basalt fibres (index K) and epoxy resin matrix (index E). Then let both phases deform elastically so that their Poisson ratio is the same and that the stresses cause no debonding of the interfaces. The volumetric ratio of basalt fibres (composite has the same length as individual phases) Φ_K .

From the simple rule of mixture (derivation is in [4]) it follows that

$$E_C = \Phi_K E_K + (1 - \Phi_K) E_E \quad (22)$$

Here E_C is the longitudinal creep modulus of linear composite, E_E is the longitudinal creep modulus of epoxy resin and E_K is the longitudinal creep modulus of basalt fibres. For known Φ_K and E_C, E_E the longitudinal compressive modulus of basalt fibres is equal to

$$E_K = [E_C - (1 - \Phi_K) E_E] / \Phi_K \quad (23)$$

For our case the Φ_K was estimated by image analysis and a value of $\Phi_K = 0.9$ was obtained. The modulus E_C at indi-

Table 4. Parameters of compressive creep.

Linear composite (C)			Basalt rod (R)	
T _T , °C	D, mm	t _{1/2} , s	D, mm	t _{1/2} , s
30	0.0030	145.1	0.0145	16015
50	0.0289	36.90	-	-
100	0.0532	29.80	0.0083	21.30
250	0.0350	41.10	-	-
300	-	-	0.0426	51.7

Table 5. Longitudinal compressive modulus of linear composite, epoxy resin and basalt fibres.

T, °C	E _K Basalt, GPa	E _C Composite, GPa	E _E Resin, GPa
25	112.27	105.41	40.5129
50	95.256	87.49	17.5076
100	114.084	108.575	58.9869
200	99.76	90.95	11.6239

vidual temperatures was computed as the ratio

$$E_C = \frac{F}{A_C \epsilon_{C(30)}} \quad (24)$$

where $F = 200$ mN is the applied load, $A_C = 20.725$ mm² is the cross sectional area of the composite sample tested and $\epsilon_{C(30)}$ is the deformation under compressive creep in time $t = 30$ s. Values $\epsilon_{C(30)}$ were computed from dimensional changes after 30 sec. of compressive creep for linear composite at individual temperatures. Modulus E_E was estimated from the compressive creep curve of pure epoxy resin in the same way. In this case $F = 200$ mN, $A_E = 20.725$ mm² and $\epsilon_{E(30)}$ were computed from dimensional changes after 30 s of compressive creep for epoxy resin at individual temperatures.

Computed values of E_E , E_C and E_K are summarized in the Table 5.

Analysis of particles emitted during basalt handling

Some characteristics of basalt fibres are similar to asbestos. Since the mechanisms for asbestos carcinogenicity are not fully known it cannot be excluded that basalt fibres may also be hazardous to health. Thus, there is a need for the analysis of fibrous fragment characteristics in production and handling in order to control their emission.

Based on the results of workshop held in April 1988 at Oak Ridge National Laboratory, fibrous fragments with diameter of 1.5 μ m or less and length of 8 μ m or greater should be handled and disposed of using the widely accepted procedures for asbestos. Fibres falling within the following three criteria are of concern [13].

- The fibres are respirable. Diameters of less than 1.5 μ m (some say less 3.5 μ m) allow fibres to remain airborne and respirable.
- The fibres have a length/diameter ratio R greater than 3. Short stubby fibres (particles) do not seem to cause the serious problems associated with asbestos.
- The fibres are durable in the lungs. If fibres are decomposed in the lungs, they do not cause a problem.

Most nonpolymeric fibres have a diameter significantly larger than 3.5 μ m, but break into long thin pieces. The Emission of particles, including fibres, occurs

during handling. For simulation of these phenomena the abrasion of basalt weaves was done.

Weave from basalt filaments was used. Fragmentation was realized by abrasion on a propeller type abrader. Time of abrasion was 60 seconds. It was proved by microscopic analysis that basalt fibres do not split and the fragments have a cylindrical shape. Fibre fragments were analysed by image analysis, using a LUCIA M system. Only fragments shorter than 1000 μ m were analysed. Results were lengths L_i of fibre fragments. For comparison the diameters D_i of fibre fragments were measured as well.

Basic statistical characteristics of the fibre fragment lengths are:

mean value $L_M = 230.51$ μ m
 standard deviation $\sigma_L = 142.46$ μ m
 skewness $g_1 = 0.969$
 kurtosis $g_2 = 3.97$.

These parameters show that the distribution of fibre fragments is unimodal and positively skewed. The same results are valid for the distribution of fibre fragment diameters.

Basic statistical characteristics of fibre fragments diameters are:

mean value $D_M = 11.08$ μ m
 standard deviation $\sigma_L = 2.12$ μ m
 skewness $g_1 = 0.641$
 kurtosis $g_2 = 2.92$.

Because the mean value of fibre fragment diameter is the same as the diameter of fibre, no splitting of fibres during fracture occurs. It is known that from the point of view of being a cancer hazard, length/diameter ratio R is very important. For basalt fibre fragments ratio

$$R = 230.51/11.08 = 20.8.$$

Despite the fact that basalt particles are too thick to be respirable, the handling of basalt fibres must be carried out with care.

Summary

In this contribution the selected thermal and mechanical properties of basalt filaments were presented. The properties were investigated after tempering at 50, 100, 200, 300, 400 and 500 °C. The ultimate strength, deformation at break, shear

modulus and sound wave spread velocity were measured. The strength distribution of basalt filaments was modeled by the three parameter Weibull type model. Thermal properties were investigated by TMA apparatus. Thermal expansion and compressive creep were measured. It was proven that a major problem with basalt fibre application is gradual crystallisation during temperature exposition. This conclusion is valid for industrially produced basalts fibres as well [12]. The shear and compressive moduli of basalt filaments are comparatively high.

The health problems with this class of fibres are not known. Very long thin fragments of basalt can be dangerous when inhaled.

Acknowledgments

This work was supported by the research project GACR 106/531/2005 and projects 1M4674788501 and 1M06 047.

References

- Douglas R.W. - Ellis B.: *Amorphous Material*. Wiley, London, 1972.
- Kopecký L. Voldán J.: *Crystallization of melted rocks*. CSAV, Prague 1959.
- Rubnerová J.: *Thermomechanical properties of inorganic fibres*. (Diploma work), TU Liberec 1996.
- Militký J. et. al.: *Proc. Int. Conf. Special Fibres*, Łódź 1997.
- Morse S. A.: *Basalts and Phase Diagrams*, Springer Verlag, New York 1980.
- Krutzky N., et al.: *Geol. Pruzkum* 22, 33. 1980.
- Slivka M., Vavro M.: *Ceramics* 40, 149. 1996.
- Wagner H. D.: *J. Polym. Sci. Phys. B27*, 115. 1989.
- Kittl P., Díaz G.: *Res. Mechanica* 24, 99. 1988.
- Meloun M., Militký J., Forina M.: *Chemometrics for Analytic Chemistry vol. I, Statistical Data Analysis*, Ellis Horwood, Chichester 1992.
- Meloun M., Militký J., Forina M.: *Chemometrics for Analytic Chemistry vol II, Regression and related Methods*, Ellis Horwood, Hempstead 1994.
- Militký J.: *Proc. 25th. Textile Research Symposium at Mt. Fuji, August 1996*.
- Weddell J.K.: *Continuous Ceramic Fibres*. *J. Text. Inst.* No.4, 333, 1990.
- Weibull W.: *J. Appl. Mech.* 8,293, 1951.
- Cran G. W.: *IEEE Trans. Reliability* 37, 360 (1988).

Received 15.11.2007 Reviewed 15.01.2008